

Hydrogen Bond versus Polar Effects: An Ab Initio Analysis on $n \rightarrow \pi^*$ Absorption Spectra and N Nuclear Shieldings of Diazines in Solution

Benedetta Mennucci*

Contribution from the Dipartimento di Chimica e Chimica Industriale, Università di Pisa, via Risorgimento 35, 56126 Pisa, Italy

Received July 30, 2001. Revised Manuscript Received October 16, 2001

Abstract: The complex nature of the effect of H-bonding solvents on electronic and magnetic properties of diazines in dilute solution is analyzed by comparing results obtained with continuum, discrete, and mixed continuum–discrete solvation methods. For comparison, other, nonprotic solvents are also considered. The interpretation of the results shows that strong H-bonding effects, such as those exerted by water molecules on diazines nitrogens, are accompanied by comparable (or at least not negligible) long-range polar interactions. It is also shown that a continuum model not only well describes such “bulk effects” but becomes essential to get the correct description of the interactions due to explicit H-bonded molecules. This double action (direct, as an additional long-range field, and indirect, through the H-bonded molecules) significantly modifies the solute electronic and nuclear charge distribution and the related response properties. This picture is confirmed by an NBO analysis on single diazines and the corresponding H-bonded clusters with and without an external continuum solvent.

1. Introduction

It is well-known that solute–solvent interactions have a significant effect on the behavior of molecular systems including nitrogen atoms. The largest sensitivity to solvent occurs when the nitrogen lone pair is involved in sp^2 -type hybridization and is available for hydrogen bonding with protic solvents. Following such evidence, in this paper we shall present a study on the environment effects on a specific class of molecular systems containing sp^2 -type nitrogens: three diazines, also known as pyridazine (1,2-diazine), pyrimidine (1,3-diazine), and pyrazine (1,4-diazine). The attention will be focused on two particular phenomena which have been shown to be very sensitive to the presence of the solvent and to the way this interacts with the molecular system: electronic absorption spectra and nitrogen NMR shieldings.

The blue shift of the lowest $n \rightarrow \pi^*$ electronic transition of diazines in solvents of various nature (in terms of polarity and proticity) has been of great interest for a long time, from both experimental^{1,2} and theoretical points of view.^{3–7} In particular, specific attention has been focused on the effects of possible

hydrogen bonding between diazine nitrogen atoms and solvent (especially water) hydrogens.

In parallel, important solvent effects have been observed on the nuclear shielding of diazine nitrogens, for which an increase of up to 40–50 ppm has been measured⁸ (we note that this is one of the largest solvent-induced shifts so far observed in nitrogen NMR and that, as shown for $n \rightarrow \pi^*$ transition, also here a large contribution has to be imputed to hydrogen-bonding effects).

Solvent effects on nuclear magnetic shielding parameters derived from NMR spectroscopy have been the subject of very important theoretical papers; here, in particular, we quote the contribution given by Buckingham.⁹ In his works, he suggested a possible classification in terms of various additive corrections to the shielding arising from the bulk magnetic susceptibility of the solvent, the magnetic anisotropy of the solvent molecules, van der Waals forces, and the “polar” effect. In the original scheme, H-bonding specific interactions were mentioned only as a possible extreme form of the “polar” effect, but in the numerous applications which followed, they have always been treated as a separate contribution. Beside this long tradition of theoretical investigation on the nature of solvent effects on NMR parameters, the literature on computational studies is by far more recent, especially if we focus on accurate ab initio calculations.^{10–12}

The availability of experimental data on different properties and the high sensitivity to solvent effects, and in particular to

* E-mail: bene@dcc.i.unipi.it.

- (1) Baba, H.; Goodman, L.; Valenti, P. C. *J. Am. Chem. Soc.* **1966**, *88*, 5410.
- (2) (a) Brealey, G. J.; Kasha, M. *J. Am. Chem. Soc.* **1955**, *77*, 4462. (b) Krishna, V. G.; Goodman, L. *J. Am. Chem. Soc.* **1961**, *83*, 2042.
- (3) (a) Zeng, J.; Hush, N. S.; Reimers, J. R. *J. Chem. Phys.* **1993**, *99*, 1482; 1495; 1508. (b) Zeng, J.; Hush, N. S.; Reimers, J. R. *J. Phys. Chem.* **1996**, *100*, 9561.
- (4) de Almeida, K. J.; Coutinho, K.; de Almeida, W. B.; Rocha, W. R.; Canuto, S. *Phys. Chem. Chem. Phys.* **2001**, *3*, 1583.
- (5) Karelson, M. M.; Zerner, M. C. *J. Phys. Chem.* **1992**, *96*, 6949.
- (6) Gao, J.; Byun, K. *Theor. Chem. Acc.* **1997**, *96*, 151.
- (7) Serrano-Andrés, L.; Fülischer, M. P.; Karlström, G. *Int. J. Quantum. Chem.* **1997**, *65*, 168.

- (8) Witanowski, M.; Stefaniak, L.; Webb, G. A. In *Annual Reports on NMR Spectroscopy*; Webb, G. A., Ed.; Academic Press: London, 1993; Vol. 25.
- (9) (a) Buckingham, A. D. *Can. J. Chem.* **1960**, *38*, 300. (b) Buckingham, A. D.; Schaefer, T.; Schneider, W. G. *J. Chem. Phys.* **1960**, *32*, 1227.

H-bonding, make diazines a challenging test for models aiming at describing solute–solvent interactions. The knowledge of solvent-induced changes on both electronic transitions and nuclear shieldings of the same molecular system, in fact, represents a rather unique opportunity to better understand the real nature of solute–solvent interactions, including H-bonding.

The number of theoretical methods developed so far to study solvation effects is large; however, it is useful to identify two distinct categories: continuum solvation models, where the solvent is considered as a macroscopic continuum dielectric characterized by its refractive index and permittivity, and discrete solvation models, where the solvent maintains its microscopic nature. In turn, each category collects very different methodologies, and sometimes the boundary between one and the other becomes very unclear. In any case, this two-category scheme is widely used, and, in particular, it becomes very effective when the main interest is on the analysis of the combined action induced by the solvent through nonspecific and long-range “polar” (or polarization) effects, on one hand, and specific and short-range interactions, on the other hand.

In this study, approaches belonging to both categories will be used and compared in order to reach a more complete understanding of the nature of the interactions acting in dilute solutions of the three diazines and, in particular, to rationalize the effects of H-bonding between a protic solvent (here water) and the proton-acceptor diazines (in which sp^2 -type nitrogen atoms constitute very effective acceptor centers).

The continuum solvation model we shall adopt here is the so-called integral equation formalism (IEF),¹³ the most recent development of the largely diffused PCM method.¹⁴ This is an accurate continuum solvation model which uses a molecular-shaped cavity to define the boundary between solute and continuum dielectric, and apparent surface charges (ASCs) to describe the electrostatic solvent effects. An important feature of this model is that solvent apparent charges depend on the solute charge distribution (here represented in terms of its wave function without additional simplifications) and, at the same time, they modify it through a perturbation operator to be added to the solute Hamiltonian: in this way, it is possible to take into account mutual polarization effects between solute and solvent.

The discrete model adopted here is represented by small clusters (the solute plus one or two H-bonded water molecules) obtained through ab initio geometry optimizations in which all

the parts of the cluster are treated at the same quantum mechanical level. In addition to these two main methods, a third, hybrid approach is introduced: H-bonded solute–solvent clusters recomputed in the presence of an external continuum dielectric (still in the framework of the IEF model).

This study can be considered as a continuation and a further development of research started with a recent paper on the effects of another protic solvent, chloroform, on nitrogen nuclear shielding of acetonitrile and pyridine.¹⁵ With respect to the scheme of analysis used in this reference study, important differences will be found in the present one focused on water. As a matter of fact, $CHCl_3$ is a protic solvent like water, but its H-donor strength is by far weaker, and thus the contribution of H-bonding to the interactions with solute cannot be well represented in terms of a single (or few) rigid structure obtained as the minimum of the potential energy surface of the corresponding solute–solvent cluster. On the contrary, the real situation is dynamic, and a variety of different and representative structures can and do occur. In the referenced paper, this situation was achieved by considering structures derived from molecular dynamics (MD) shots taken at different simulation times. In contrast, previous studies performed by other groups (both experimentally and theoretically) on water–diazine system have shown that this time H-bonding interactions are strong enough to give stable clusters which can be thus described as really existing systems.

The study will be organized as follows: in the first part we shall describe $n \rightarrow \pi^*$ absorption spectra of the three diazines and the way they are modified by solvent; besides water, another polar but not protic solvent (acetonitrile) will also be reported, although the analysis in terms of solute–solvent clusters will be limited to water. The second part of the paper will present and discuss the results obtained for nitrogen nuclear shielding. Also for this property, results for three other solvents besides water will be presented, namely cyclohexane, acetone, and dimethyl sulfoxide; still, the cluster study will be limited to water solution. For both properties, an orbital-based study exploiting a natural bond orbital (NBO) analysis will be used to rationalize the computed results.

2. Computational Details

Geometry optimizations for all the systems (single diazines and H-bonded clusters) both in vacuo and in the various solvents were performed on the basis of the density functional theory (DFT) using the hybrid functional which mixes the Lee, Yang, and Parr functional for the correlation part and Becke’s three-parameter functional for the exchange (B3LYP). The basis set used was the 6-31+G(d,p). We note that density functional methods have recently proved quite useful to study hydrogen-bonded complexes. The B3LYP functional in particular has proven effective, at least as long as basis sets no less than 6-31+G(d,p) are used and electrostatic interactions play a dominant role; in fact, there is reason to believe that density functional theory is generally not appropriate for generalized van der Waals complexes in which dispersion interactions are predominant.¹⁶

To evaluate absorption transition energies, the time-dependent density functional theory (TDDFT) was used with the same basis set exploited

- (10) (a) Chesnut, D. B.; Rusiloski, B. E. *J. Mol. Struct.: THEOCHEM* **1994**, *314*, 19; *114*, 1604. (b) Mikkelsen, K. V.; Jørgensen, P.; Ruud, K.; Helgaker, T. *J. Chem. Phys.* **1997**, *106*, 1170. (c) Pecul, M.; Sadlej, J. *J. Chem. Phys.* **1998**, *234*, 111. (d) Zhan, C. G.; Chipman, D. M. *J. Chem. Phys.* **1999**, *110*, 1611. (e) Yamazaki, T.; Sato, H.; Hirata, F. *Chem. Phys. Lett.* **2000**, *325*, 668.
- (11) Witanowski, M.; Biedrzycka, Z.; Sicinska, W.; Grabowski, Z.; Webb, G. A. *J. Magn. Reson.* **1997**, *124*, 127. Witanowski, M.; Sicinska, W.; Biedrzycka, Z.; Webb, G. A. *J. Mol. Struct.* **1999**, *476*, 133. Witanowski, M.; Biedrzycka, Z.; Sicinska, W.; Grabowski, Z. *J. Magn. Reson.* **1998**, *131*, 54. Witanowski, M.; Sicinska, W.; Biedrzycka, Z.; Webb, G. A. *Magn. Reson. Chem.* **2000**, *38*, 177. Jaszunski, M.; Mikkelsen, K. V.; Rizzo A.; Witanowski, M. *J. Phys. Chem. A* **2000**, *104*, 1466. Witanowski, M.; Biedrzycka, Z.; Sicinska, W.; Webb, G. A. *J. Mol. Struct.* **2000**, *516*, 107. Witanowski, M.; Biedrzycka, Z.; Grabowski, Z. *Magn. Reson. Chem.* **2000**, *38*, 580.
- (12) (a) Cammi, R. *J. Chem. Phys.* **1998**, *109*, 3185. (b) Cammi, R.; Mennucci, B.; Tomasi, J. *J. Chem. Phys.* **1999**, *110*, 7627.
- (13) (a) Cancès, E.; Mennucci, B. *J. Math. Chem.* **1998**, *23*, 309. (b) Cancès, E.; Mennucci, B.; Tomasi, J. *J. Chem. Phys.* **1997**, *107*, 3031. (c) Mennucci, B.; Cancès, E.; Tomasi, J. *J. Phys. Chem. B* **1997**, *101*, 10506.
- (14) (a) Miertus, S.; Scrocco, E.; Tomasi, J. *J. Chem. Phys.* **1981**, *55*, 117. (b) Cammi, R.; Tomasi, J. *J. Comput. Chem.* **1995**, *16*, 1449.

- (15) Mennucci, B.; Martínez, J. M.; Tomasi, J. *J. Phys. Chem. A* **2001**, *105*, 7287.
- (16) (a) Wesolowski, T. A.; Parisel, O.; Ellinger, Y.; Weber, J. *J. Phys. Chem. A* **1997**, *101*, 7818. (b) Meijer, E. J.; Sprik, M. *J. Chem. Phys.* **1996**, *105*, 8684. (c) Hobza, P.; Sponer, J.; Reschel, T. *J. Comput. Chem.* **1995**, *16*, 1315. (d) Kristyan, S.; Pulay, P. *Chem. Phys. Lett.* **1994**, *229*, 175. (e) Rablen, P. R.; Lockmann, J. W.; Jørgensen, W. L. *J. Phys. Chem. A* **1998**, *102*, 3782.

to get geometries. Calculations of nuclear shieldings were performed at the B3LYP level, exploiting the gauge-including atomic orbital (GIAO) method.¹⁷ For all systems, the same geometries used to get absorption were adopted, as well as the same hybrid functional B3LYP, whereas the basis set was enlarged to 6-311+G(d,p). All ab initio calculations both in vacuo and in solution were performed using a development version of the Gaussian code.¹⁸

Solvation. In the IEF-PCM solvation model,¹³ the solvent is mimicked by a dielectric continuum with dielectric constant ϵ , surrounding a cavity with shape and dimension adjusted on the basis of the real geometric structure of the solute molecule. The latter polarizes the solvent, which, as a response, induces an electric field (the “reaction field”) which interacts with the solute. In the IEF model, the electrostatic part of such an interaction is represented in terms of an apparent charge density spread on the cavity surface, which gives rise to a specific operator to be added to the Hamiltonian of the isolated system to obtain the final effective Hamiltonian and the related Schrödinger equation. Solvent terms depend on the solute wave function they contribute to modify, and thus the problem requires the solution of a proper SCF scheme.

This is the general approach in which solute electronic and nuclear charge distribution and solvent reaction field can mutually equilibrate; however, in vertical electronic transitions, the relaxation of the reaction field in the direction of the new solute electronic state may be incomplete. If we take into account the typical time scales characterizing electronic and nuclear (or molecular) motions, we can safely assume that only the part of the solvent reaction which is induced by the polarization of its electrons can immediately modify according to the new electronic state reached by the solute in the transition process; all the rest remains frozen in the previous equilibrium condition determined by the initial state. To a reasonable approximation, the fast component can be taken as proportional to the dielectric constant at infinite frequency ϵ_∞ , where $\epsilon_\infty \approx n^2$ and n is the refractive index of the solvent. In the framework of IEF-PCM, this scheme is realized by introducing two sets of apparent charges representing the electronic (or fast) and the slow contributions of the solvent reaction, respectively.¹⁹

IEF-PCM has been recently generalized to both TDDFT calculations and the GIAO method so as to include solvent perturbation operators in the two coupled perturbed schemes; for more details on the formalisms, see refs 20 and 12.

In the IEF-PCM model, the molecular cavity is obtained in terms of interlocking spheres centered on selected nuclei. The chosen radii are 1.9 Å for the aromatic carbons bonded to a hydrogen atom, 1.6 Å for all N, 1.52 Å for O, and 1.2 Å for H of H-bonded water.²¹ All the radii have been multiplied by a factor (equal to 1.2 if not otherwise specified) in order to take into account the fact that atomic bonds or lone pair centers of the solvent molecules are normally located a bit farther from the solute atoms than a van der Waals radius.²² For all solvents, it is necessary to define the macroscopic permittivity (two values, ϵ and ϵ_∞ , are required in absorption calculations); the values used in the following calculations are 78.39 (and 1.776) for water, 36.64

Table 1. Experimental and Computed TDDFT (B3LYP/6-31+G(d,p)) Absorption Energies (eV) of Diazines in Vacuo (VAC), in Acetonitrile (ACN), and in Water (H₂O)^a

	pyridazine			pyrimidine			pyrazine		
	VAC	ACN	H ₂ O	VAC	ACN	H ₂ O	VAC	ACN	H ₂ O
$n \rightarrow \pi^*$	3.58	3.86	3.87	4.29	4.42	4.43	3.97	4.00	4.01
exp ^b	3.6 ^c	3.85	4.16	4.2 ^c	4.32	4.57	3.9 ^c	3.94	4.11
$\delta_{n\pi^*}$	0	0.28	0.29	0	0.13	0.14	0	0.03	0.04
$\delta_{n\pi}^{exp}$	0	0.25	0.56	0	0.12	0.37	0	0.04	0.21

^a For all solutions the IEF model has been used. ^b Reference 1. ^c In isooctane.

(and 1.806) for acetonitrile, 46.70 for dimethyl sulfoxide (DMSO), 20.70 for acetone, and 2.023 for cyclohexane.

3. Electronic Absorption

The experimental $n \rightarrow \pi^*$ electronic transition of dilute diazines in different solvents has long been of interest.² Baba and co-workers¹ measured the $n \rightarrow \pi^*$ fluorescence and excitation spectra as well absorption spectra for the three diazines in isooctane, ether, acetonitrile, methanol, and water. From these measurements it appeared that, for protic solvents, hydrogen bonds between solute and solvent molecules give rise to a large blue shift in the absorption transition, but they have practically no effect upon the $n \leftarrow \pi^*$ fluorescence transition. The authors thus concluded that the hydrogen bond is broken in the ($n\pi^*$) singlet excited state.

From the same study comes an important and still open aspect, namely the relevant question about what fraction of the observed solvent shifts can be attributed to specific H-bond interactions and what fraction can be attributed to nonspecific solvation effects. The differences observed by Baba et al. for the three diazines in various solvents suggest that, in protic solvents (like water and methanol), a minor, but still significant part (from one-fifth for pyrazine to one-half for pyridazine) of the observed absorption solvent shifts is due to nonspecific solvation, while the rest is due to hydrogen bonding.

To try to confirm or discard this finding, in Table 1 we report the results of our calculations (TDDFT B3LYP/6-31+G(d,p)) on the absorption energies for the three diazines in vacuo and in the two polar solvents. The geometries have been reoptimized in each phase.

An aspect to be preliminarily considered in order to perform a more correct analysis of solvent effects is the check on the quality of the quantum mechanical level of calculation in relation to the phenomenon under scrutiny. This check can be more easily achieved by considering isolated systems (for which no approximations due to the solvent model are introduced): the results reported in Table 1 for gas-phase diazines show that, for all three molecules, the agreement between computed and experimental absorption energies is very good. We recall that the gas-phase experimental absorption energies (and the following shifts in the two solvents) reported in Table 1 are actually measured in isooctane: the very low polarity of this solvent ($\epsilon = 1.933$), however, ensures the validity of this approximation. This good accord obtained for the isolated systems make us sufficiently confident in the accuracy of the TDDFT (B3LYP/6-31+G(d,p)) level to describe this specific electronic transition and thus to ensure a reliable analysis of solvent effects on the same transition.

If we now compare the results obtained in the two polar solvents, it is evident that for acetonitrile, where no hydrogens

- (17) (a) Hameka, H. F. *Rev. Mod. Phys.* **1962**, *34*, 87. (b) Ditchfield, R. *Mol. Phys.* **1974**, *27*, 789. (c) Wolinski, K.; Hinton, J. F.; Pulay, P. *J. Am. Chem. Soc.* **1990**, *112*, 8251.
- (18) Frisch, M. J.; Trucks, G. W.; Schlegel, H. B.; Scuseria, G. E.; Robb, M. A.; Cheeseman, J. R.; Zakrzewski, V. G.; Montgomery, J. A., Jr.; Stratmann, R. E.; Burant, J. C.; Dapprich, S.; Millam, J. M.; Daniels, A. D.; Kudin, K. N.; Strain, M. C.; Farkas, O.; Tomasi, J.; Barone, V.; Cossi, M.; Cammi, R.; Mennucci, B.; Pomelli, C.; Adamo, C.; Clifford, C. S.; Ochterski, J.; Petersson, G. A.; Ayala, P. Y.; Cui, Q.; Morokuma, K.; Malick, D. K.; Rabuck, A. D.; Raghavachari, K.; Foresman, J. B.; Cioslowski, J.; Ortiz, J. V.; Stefanov, B. B.; Liu, G.; Liashenko, C. A.; Piskorz, P.; Komaromi, I.; Gomperts, R.; Martin, R. L.; Fox, D. J.; Keith, T.; Al-Laham, M. A.; Peng, C. Y.; Nanayakkara, A.; Gonzalez, C.; Challacombe, M.; Gill, P. M. W.; Johnson, B.; Chen, W.; Wong, M. W.; Andres, J. L.; Head-Gordon, M.; Replogle, E. S.; Pople, J. A. *Gaussian 99*, Development Version; Gaussian Inc.: Pittsburgh, PA, 1999.
- (19) Cammi, R.; Mennucci, B.; Tomasi, J. *J. Chem. Phys.* **1998**, *109*, 2798.
- (20) Cammi, R.; Mennucci, B.; Tomasi, J. *J. Phys. Chem. A* **2000**, *104*, 5631.
- (21) Bondi, A. J. *J. Phys. Chem.* **1964**, *68*, 441.
- (22) Tomasi, J.; Persico, M. *Chem. Rev.* **1994**, *94*, 2027.

Table 2. TDDFT (B3LYP/6-31+G(d,p)) Absorption Energies (eV) of Water–Diazine Clusters in Vacuo (VAC) and in the Presence of an External Continuum Dielectric (IEF)^a

	pyridazine				pyrimidine				pyrazine			
	VAC		IEF		VAC		IEF		VAC		IEF	
	+1w	+2w	+1w	+2w	+1w	+2w	+1w	+2w	+1w	+2w	+1w	+2w
$n \rightarrow \pi^*$	3.74	3.85	4.00	4.13	4.40	4.53	4.50	4.61	4.02	4.08	4.06	4.13
geom _v			3.98	4.08			4.53	4.63			4.08	4.15
$\delta_{n\pi^*}$	0.16	0.27	0.42	0.55	0.11	0.24	0.21	0.32	0.05	0.11	0.09	0.16
$\delta_{n\pi^*}^{\text{exp}}$		0.56				0.37				0.21		

^a The row indicated as “geom_v” refers to IEF calculations performed on the gas-phase geometries. Experimental shifts are from ref 1.

are available to interact with diazine nitrogens, the IEF continuum model gives very good gas-to-solution shifts for all molecules. In contrast, for water the agreement with experimental data significantly worsens: the computed shift reproduces only a part (going from one-fifth for pyrazine to one-half for pyridazine) of the whole observed effect. The missing term (almost constant in all molecules and around 0.2 eV) is clearly due to H-bonding which, according to the analysis given by Baba et al., induces an additional blue shift due to the energy of the hydrogen bond formation in the ground state.

The good results obtained in acetonitrile also confirm that, for this particular electronic transition, effects due to solute–solvent nonelectrostatic interactions (generally indicated as van der Waals) are not important, and thus the electrostatic continuum model correctly reproduces the experimental data: different considerations will apply in the following analysis on N nuclear shieldings.

3.1. Water–Diazine Clusters. To test the validity of the analysis we have derived from Table 1 on the relative contributions of H-bonding and “polar” effects, we have optimized two H-bonded clusters containing one and two water molecules, respectively, without and with an external continuum dielectric. On such optimized geometries, we have computed TDDFT transition energies at the same level (B3LYP/6-31+G(d,p)) used before for the single diazines. The computed results are reported in Table 2.

From the results obtained for both isolated and “solvated” (in the sense of adding a IEF continuum) clusters, it seems evident that the most realistic picture, i.e., that giving results closer to experiments, is that with two simultaneous H-bonds (one on each nitrogen): this confirms previous theoretical³ and experimental data.²³ Here, however, a further aspect comes out clearly: even by taking into account the two H-bonds, an important portion of the observed shift is still missing. For all molecules, in fact, the isolated “diazine + 2 waters” clusters seem not able to describe the complete effect due to the whole liquid. Adding an external continuum, i.e., including also long-range nonspecific polarization effects, fills the missing gap and leads to a very good agreement with experiments.

For a more complete interpretation of the effect, in Table 2 we also report IEF continuum calculations on the structures optimized in vacuo (see row indicated as “geom_v”): these calculations should allow us to extract the solvent-indirect effect due to geometry relaxation. By comparing these results with the previous ones obtained with reoptimized structures, we can see that for all systems geometry relaxation effects are very

Table 3. NBO Analysis on Pyridazine and Water–Pyridazine Clusters in Vacuo (VAC) and in the Presence of an External Continuum (IEF): Nitrogen Lone Pair Natural Population (NP(lp)) and Energy ($E(\text{lp})$ in kcal/mol), OH Bond Natural Population (NP(bd(OH))), and Lone Pair/OH Antibonding Stabilization Energy ($\Delta E(\text{lp}/\text{bd}_{\text{OH}}^*)$ in kcal/mol)

	VAC			IEF		
	m	+1w	+2w	m	+1w	+2w
NP(lp)	1.939	1.921	1.922	1.943	1.912	1.912
$E(\text{lp})$	−0.38	−0.40	−0.42	−0.39	−0.41	−0.41
NP(bd(OH))		1.998	1.998		1.998	1.998
$\Delta E(\text{lp}/\text{bd}_{\text{OH}}^*)$		9.59	9.35		14.74	14.20

small (almost negligible); this confirms that almost all the effect due to including an external continuum is related to a polarization of the solute charge density.

As further analysis on the real nature of the specific and nonspecific effects acting between diazines and water solvent, we introduce a NBO study²⁷ on the ground states of the clusters: for this analysis we have preferred to reduce the numbers to those of a single system (pyridazine or 1,2-diazine, which shows the largest solvent shift) so as to have a reasonably limited number of data to interpret; in any case, we recall that all the conclusions we shall obtain for pyridazine similarly apply to the two other diazines.

In Table 3 we report a selection of NBO ground-state results for the four pyridazine clusters and for the corresponding monomers. The last row in Table 3 summarizes the second-order perturbative estimates of “donor–acceptor” (bond–antibond) interactions in the NBO basis applied to the couple (lone pair/OH antibond). Since these interactions lead to loss of occupancy from the localized NBOs of the idealized Lewis structure into the empty non-Lewis orbitals (and, thus, to departures from the idealized Lewis structure description), they are referred to as “delocalization” corrections. For the donor NBO (i) and the acceptor NBO (j), the stabilization energy $\Delta E(i,j)$ associated with delocalization (“2e stabilization”) $i \rightarrow j$ is estimated as

$$\Delta E(i,j) = q_i(F(i,j)^2)/(\epsilon_j - \epsilon_i)$$

where q_i is the donor orbital occupancy, ϵ_j and ϵ_i are diagonal elements (orbital energies), and $F(i,j)$ is the off-diagonal NBO Fock matrix element.

As expected on passing from the isolated molecule (m) to the H-bonded clusters (+nw), the character of the lone pair

(23) (a) Carrabba, M. M.; Kenny, J. E.; Moomaw, W. R.; Cordes, J.; Denton, M. *J. Phys. Chem.* **1985**, *89*, 674. (b) Spencer, N. N.; Holmboe, E. S.; Kirshenbaum, M. R.; Barton, S. W.; Smith, K. A.; Wolbach, W. S.; Powell, J. F.; Chorazy, C. *Can. J. Chem.* **1982**, *60*, 1184.

(24) Witanowski, M.; Sicinska, W.; Biernat, S.; Webb, G. A. *J. Magn. Reson.* **1991**, *91*, 289.
 (25) Pople, J. A. *Discuss. Faraday Soc.* **1962**, *34*, 7.
 (26) Karplus, M.; Pople, J. A. *J. Chem. Phys.* **1963**, *38*, 2803.
 (27) Glendening, E. D.; Reed, A. E.; Carpenter, J. E.; Weinhold, F. NBO version 3.1.

Table 4. Experimental and Computed (B3LYP/GIAO/6-311+G(d,p)) Isotropic N Nuclear Shielding (in ppm) and Cyclohexane-to-Solution Shifts ($\delta\sigma_{\text{cyc}}$) of Diazines in Vacuo and in Various Solvents^a

	pyridazine				pyrimidine				pyrazine			
	exp		calc		exp		calc		exp		calc	
	$\Delta\sigma$	$\delta\sigma_{\text{cyc}}$	σ	$\delta\sigma_{\text{cyc}}$	$\Delta\sigma$	$\delta\sigma_{\text{cyc}}$	σ	$\delta\sigma_{\text{cyc}}$	$\Delta\sigma$	$\delta\sigma_{\text{cyc}}$	σ	$\delta\sigma_{\text{cyc}}$
vac			-216.94				-76.88				-118.84	
cyc	-35.31	0	-204.97	0	+80.30	0	-72.70	0	+42.17	0	-114.42	0
acetone	-25.85	9.46	-187.70	17.27	+83.41	3.11	-66.86	5.84	+44.88	2.71	-109.56	4.86
DMSO	-20.93	14.38	-186.14	24.34	+83.90	3.60	-66.26	4.89	+45.34	3.17	-108.99	5.43
water	+6.24	41.55	-185.54	19.43	+97.14	16.84	-66.35	6.35	+59.02	16.85	-108.84	5.58

^a Experimental shieldings from ref 24 are reported with respect to neat liquid nitromethane, and they are indicated as $\Delta\sigma$.

significantly changes: its population decreases (with a parallel increase in the population of the OH bond of water) and its stabilization energy increases. Both of these aspects indicate a strong H-bonding interaction. The analysis, however, becomes more interesting when the comparison between isolated and “solvated” (in the sense of the IEF continuum model) is introduced.

For each cluster, we see that adding a continuum dielectric leads to an important variation: the “lone pair/OH antibonding” delocalization energy significantly increases with respect to that found for the isolated systems. Smaller effects are found in the lone pair occupation (which slightly decreases) and energy. All these aspects contribute to indicate that including long-range effects of a continuum dielectric induces a displacement of pyridazine ground-state charge, leading to a more partially negative nitrogen atom on one hand, and to stronger H-bonding interactions with the water molecules on the other hand.

If we now consider that, when the cluster undergoes an electronic transition transferring electrons between the nitrogen lone pair and the ring antibonding π^* orbital, the stabilizing effect due to H-bonding is largely canceled, the result is that its excited state cannot be stabilized as the ground state and the absorption energy increases with respect to that of the isolated monomer. Following what was found in the previous analysis, we can guess that such an effect should be further amplified in the presence of a continuum: in this case; in fact, the stabilization of the H-bonded ground state of the cluster is larger due to the additional effects of the long-range interactions of the dielectric, while no parallel stabilization applies to the final electronic excited state. As a matter of fact, the blue shift we obtain is significantly larger in the “solvated” than in the isolated two-water (2w) clusters. Clear evidence of this behavior can be observed for pyrazine, in which the net dipole is zero, and thus the solvent effect on the $n \rightarrow \pi^*$ transition is very small also in polar but aprotic solvents (here acetonitrile): both electronic states are, in fact, almost equally stabilized by the solvent. In contrast, allowing for the possibility of H-bonds leads to important differences in the nature of the two electronic states, and in particular, it largely stabilizes the ground state; the final result is a significant shift (~ 0.2 eV).

This differential stabilizing effect on ground and excited states can be fully described only by including the effects of specific H-bond interactions together with the long-range field of the whole liquid: this, according to our calculations, can be correctly represented in terms of a continuum dielectric.

4. Nitrogen Nuclear Shielding

Solute–solvent interactions may have an important effect on the nuclear shielding of nitrogen atoms, and this effect can be

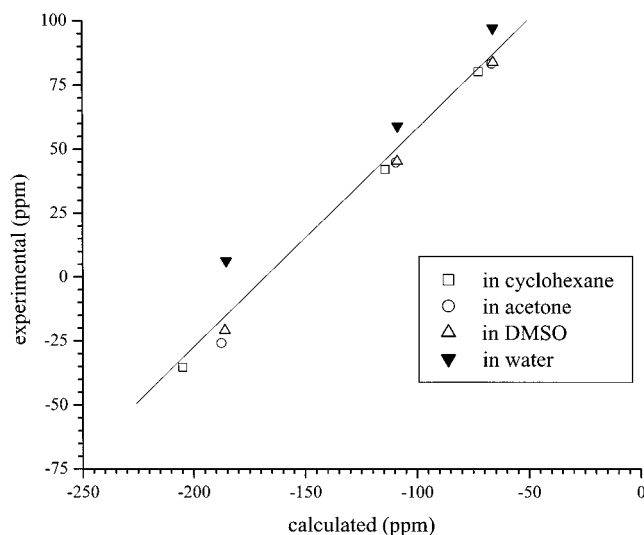


Figure 1. Experimental and B3LYP/GIAO/6-311+G(d,p) isotropic N nuclear shielding plot of diazines in various solutions. The calculated results are obtained with the IEF continuum model and standard cavities. Experimental data are reported with respect to neat liquid nitromethane.

further amplified when a nitrogen lone pair is involved in sp^2 -type hybridization and is available for hydrogen bonding with protic solvents; such behavior has also been observed in diazines.^{8,24}

In particular, for diazines, the solvent-induced shielding changes appear to be strongly dependent upon the relative positions of the two nitrogen atoms: an extreme situation is exhibited by 1,2-diazine, where, as reported above, the water-to-cyclohexane shift amounts to about 41 ppm; this represents one of largest nitrogen shielding changes so far found to be dependent upon a variation in solvent, with the exception of the case of a complete proton transfer occurring between solvent and solute.

In Table 4 we report the computed (GIAO B3LYP/6-311+G(d,p)) nitrogen shielding for the three diazines in the gas phase and in the four solutions (cyclohexane, acetone, DMSO, and water) within the framework of the IEF continuum model. In the same table we also report the experimental data in the four solutions with respect to liquid nitromethane.

To get a meaningful comparison between computed absolute shieldings and experimental relative values, in Table 4 we also report the experimental and computed cyclohexane-to-solution shifts $\delta\sigma_{\text{cyc}} = \sigma(\text{in a given solution}) - \sigma(\text{in cyclohexane})$, and in Figure 1 we report the experimental–calculated correlation plot and the line resulting from a linear fitting.

From the analysis of the shifts $\delta\sigma_{\text{cyc}}$ and from the correlation plot (the overall standard deviation is ± 9.15 ppm and the

Table 5. Isotropic N Nuclear Shielding and Shifts $\delta\sigma$ (in ppm) of Pyridine in Vacuo and in Various Solvents^a

	vac	cyc	DMSO	H
σ	-103.17	-96.16	-86.42	-86.18
$\delta\sigma_{\text{vac}}$		7.01	16.75	16.99
$\times 1.4$		4.6	9.83	9.96
$\delta\sigma_{\text{vac}}^{\text{exp}}$		3.1	8.5	29.7

^a The two sets of computed results in solution correspond to two different cavities (the standard one and that obtained with a 1.4 scaling factor). Experimental gas-phase and solution data (from which the shifts $\delta\sigma_{\text{vac}}^{\text{exp}}$ are obtained) are from ref 8.

correlation coefficient is 0.98238), it is clear that the model exploited to represent the solvent effects is incomplete; however, different considerations apply to the four different solutions (the apolar cyclohexane, the two polar but nonprotic acetone and dimethyl sulfoxide, and the polar and protic water).

The first aspect to take into account regards van der Waals effects (mainly dispersive and repulsive interactions) between solute and solvent, which have been completely neglected in the calculations giving the results reported in Table 4 (and in the corresponding plot).

The consequences of this approximation (which for the previous $n\pi^*$ transition seemed not to affect too much the results) are better quantified in a similar system (pyridine) for which real gas-phase experimental data are available (for diazine the experimental reference is a dilute cyclohexane solution, and thus a refined analysis of solvent effects is more difficult). Calculated and observed shieldings for pyridine are reported in Table 5 (the calculations have been performed at the same level as those on diazines: B3LYP/6-31+G(d,p) geometry optimizations and GIAO B3LYP/6-311+G(d,p) shielding calculations). As an example of polar nonprotic solvent, we consider here only DMSO, as no experimental data are available for acetone.

By comparing gas-to-solution computed and experimental shifts, it is evident that nonelectrostatic effects are not negligible: for the two nonprotic solvents, the computed gas-to-solution shift, $\delta\sigma_{\text{vac}}$, resulting from the electrostatic-only solvation model overestimates the observed $\delta\sigma_{\text{vac}}^{\text{exp}}$ by more than twice the value. From these results, it appears that solvent nonelectrostatic effects on nitrogen shielding induce changes in the opposite direction with respect to the electrostatic ones, and thus neglecting them leads to too-large upfield shifts in the shielding. In water the situation is largely complicated by the effects of hydrogen bonding, which prevent a reliable evaluation of nonelectrostatic effects.

Following these considerations, a very simple but still effective way to improve the agreement between calculations and experiments can be obtained by slightly enlarging the molecular cavity used in the continuum model. A larger cavity, in fact, reduces the electrostatic effects; thus, it indirectly takes into account the opposite effects due to nonelectrostatic interactions. In Table 5, the shift values reported in the row indicated " $\times 1.4$ " have been obtained with a cavity in which the radius of each van der Waals sphere has been scaled by a factor of 1.4 instead of the standard 1.2. Here, it is important to stress that this rescaling, chosen on the basis of simple qualitative considerations, does not represent a universal rule; the determination of such a rule, in fact, would require a complete fitting procedure on many different systems, which is far beyond the scope of the present paper.

Table 6. B3LYP/GIAO/6-311+G(d,p) Isotropic N Nuclear Shieldings and Gas-to-Solution Shifts $\delta\sigma_{\text{cyc}}$ (in ppm) of Diazines in Various Solvents^a

	pyridazine		pyrimidine		pyrazine	
	σ	$\delta\sigma_{\text{cyc}}$	σ	$\delta\sigma_{\text{cyc}}$	σ	$\delta\sigma_{\text{cyc}}$
cyc	-208.45	0	-74.08	0	-116.22	0
acetone	-197.19	11.26	-71.82	2.26	-114.28	1.94
DMSO	-196.16	12.29	-71.47	2.61	-113.96	2.26
water	-195.74	12.71	-71.35	3.60	-113.89	2.33

^a The computed results have been obtained with a larger cavity (i.e., using with a 1.4 scaling factor for the radii instead of the standard 1.2).

Table 7. Computed Isotropic N Nuclear Shieldings and Shifts $\delta\sigma$ (in ppm) of Water–Diazine Clusters in Vacuo (VAC) and in the Presence of an External Continuum Dielectric (IEF)^a

	VAC		IEF		exp
	+1w	+2w	+1w	+2w	
Pyridazine					
σ	-188.02	-178.16 (-191.29)	-166.53	-159.02 (-166.54)	
$\delta\sigma_{\text{cyc}}$	25.44	35.30 (17.16)	41.92	49.43 (41.91)	41.55
Pyrimidine					
σ	-61.88	-62.80	-54.72	-58.15	
$\delta\sigma_{\text{cyc}}$	13.62	12.70	19.36	15.93	16.84
Pyrazine					
σ	-98.58	-104.07	-91.65	-97.67	
$\delta\sigma_{\text{cyc}}$	18.46	12.97	24.57	18.55	16.85

^a For the two-water clusters of pyridazine, two values referring to the two nonequivalent nitrogens are reported. IEF values have been obtained with a larger cavity (obtained with a 1.4 scaling factor for the radii). Experimental data are from ref 24.

With the new enlarged cavity, the agreement between calculated and experimental gas-to-solution shifts becomes much better for both cyclohexane and DMSO; in contrast, a parallel improvement is not found for water as, for this solvent, hydrogen bond effects are so large as to reverse the situation (in fact, the electrostatic model alone also underestimates the real effect).

If we now apply the same considerations to the three diazines and we use a similarly enlarged cavity (i.e., where the radius of each van der Waals sphere has been scaled by a factor of 1.4 instead of the standard 1.2), we obtain the results reported in Table 6.

Such an enlarged cavity significantly improves the agreement between computed and experimental data for all nonprotic solvents as quantified in terms of the corresponding gas-to-solution shifts $\delta\sigma_{\text{cyc}}$ (which have to be compared with the experimental ones reported in Table 4); such an improvement does not apply to water solution, for which a different specific analysis is required.

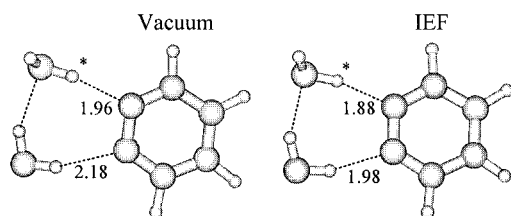
4.1. Water–Diazine Clusters. As for the previous discussion on $n \rightarrow \pi^*$ transitions, here we introduce diazine–water clusters to describe specific H-bonding effects. In Table 7 we report the calculated shieldings of the clusters without (VAC) and with the external continuum (IEF) and the corresponding cyclohexane-to-solution shifts (the IEF results are obtained with the enlarged cavity). For the clusters with just one water molecule, the shielding we report refers to the H-bonded nitrogen, as the other nitrogen behaves as in the monomers (see Tables 4 and 6).

The results presented in Table 7 confirm the analysis done on electronic transitions: including only specific H-bonding

effects (i.e., considering gas-phase clusters) means to take into account only a part of the total solvent effect, while the complete description is reproduced by adding long-range effects (here represented by the external continuum).

Before discussing in further detail such finding, it is interesting to note a specificity of this property. Contrary to what is observed for the trend in the $n \rightarrow \pi^*$ shift on passing from 1w to 2w clusters, here, considering only one H-bond leads to a larger effect than assuming a completely saturated 2w cluster. Only in pyridazine clusters, shielding behaves similarly to the $n \rightarrow \pi^*$ transition, thus indicating that for this molecule the effects of the two H-bonds are additive: this diversity of pyridazine with respect to the other diazines needs further analysis.

Pyridazine is characterized by the aggregation of two nitrogen atoms in adjacent ring positions: this vicinity affects the structure of the two-water cluster which presents an asymmetry between the two H-bonds and thus makes the two nitrogens not completely equivalent. In the scheme below we report the structures obtained in vacuo and in solution with the HOH...N distances (in Å).



The nonequivalence of the two nitrogens is reflected in the corresponding shieldings which differ by about 13 ppm in vacuo and 6 ppm in solution (see the two values reported in Table 7 for each 2w cluster, the first one referring to the nitrogen with the closest hydrogen, that indicated with the asterisk in the scheme above). This aspect has to be taken into account in the comparison with the experimental cyclohexane-to water shift: pyridazine is, in fact, the system for which we observe the largest computed–observed discrepancy and the only one for which the 1w cluster gives a better result than the 2w cluster. It is worth noting that such a trend is changed by considering the other nitrogen in the 2w cluster (the corresponding values are reported between parentheses in Table 7): in this case, the shift with respect to cyclohexane reduces to 41.91 ppm, while the experimental value is 41.55 ppm.

For the clusters, it is also interesting to check the effects due to geometry relaxations: as done for the analysis on the $n \rightarrow \pi^*$ transition, also here, for the solvated clusters, we have recomputed shieldings and shifts using the geometries obtained for the isolated systems. This time, the effects are not completely negligible (between 5 and 10% on the shifts), thus indicating a far larger sensitivity of nuclear shielding to geometrical parameters with respect to electronic transitions. This aspect is quite important, as it indicates that computational studies on nitrogen (or other nuclei) shieldings have to pay a great amount of attention to the definition of the geometrical structures; for clusters in particular, this becomes a very delicate issue which always needs a detailed analysis.

The data reported in Table 7 have introduced important aspects, but they still prevent a more detailed interpretation of the competitive/synergic action of short-range and specific

interactions on one side, and long-range and mediated effects on the other side. This can be achieved by reconsidering the previous NBO analysis done on pyridazine and extending it to all the monomers and the clusters in vacuo and in water.

4.1.1. Paramagnetic Term and NBO Analysis. It has been observed that shift trends for nitrogen shielding in different environments arise almost entirely from variations in the local paramagnetic contribution, the corresponding local diamagnetic term being almost constant.⁸ We recall that diamagnetic nuclear shielding arises from circulation of electrons in the *s* orbitals and filled shells surrounding the nucleus and is dependent on the ground state of the molecule. The diamagnetic contribution to chemical shielding is normally associated with increased shielding, with the local field at the nucleus antiparallel to the external magnetic field. Paramagnetic shielding, which arises from the nonspherical orbitals, is associated with the orbital angular momentum of electrons and is therefore dependent on excited states of the molecule. Paramagnetic contributions normally result in deshielding. More in particular, the local paramagnetic contribution can be interpreted in terms of electronic properties by applying the shielding model originally developed by Pople;²⁵ according to this model, variations in nuclear shielding of an atom A can be related to changes in its local charge densities, bond orders, and energies of electronically excited states:²⁶

$$\sigma_A^p(\text{loc}) = -\frac{\mu_0 \hbar^2 e^2}{8\pi m^2} \frac{1}{\Delta E} \langle r^{-3} \rangle_{2p} \sum_B Q_{AB} \quad (1)$$

where the summation over nucleus B includes A and Q_{AB} involves elements of the charge density–bond order matrix, ΔE is the average excitation energy (AEE), and $\langle r^{-3} \rangle_{2p}$ is the mean inverse cube of the radius of the 2p orbitals on the atom containing nucleus A.

If we apply this scheme to the interpretation of H-bonds' effects on diazines, the attention has to be focused on N lone pair orbitals. When these are not directly involved in the H-bonds and a π -electron system is available for low-energy $n \rightarrow \pi^*$ transitions (as is the case in free diazines), a large (negative) paramagnetic term will be found. In contrast, the partial removal of the lone pair from nitrogen due to H-bonding interactions with the solvent will reduce this $n \rightarrow \pi^*$ contribution and the absolute magnitude of the paramagnetic term. As a final result, a net increase in the total nuclear shielding will be observed. This is exactly what should happen in diazines passing from gas-phase (or apolar and aprotic solvents) to protic solvents.

To rationalize the results presented in Table 7 according to this interpretative scheme, in Table 8 we report the isotropic component of the paramagnetic and diamagnetic shielding tensor, σ_{is}^p and σ_{is}^d , and NBO lone pair occupations for the monomers and the clusters in gas phase (VAC) and in the continuum (IEF) (for pyridazine, two values referring to the two nonequivalent nitrogens are reported).

Results reported in Table 8 show that changes in diamagnetic terms are not negligible on passing from the monomer to the clusters, while they are small on going from the 1w to the 2w clusters; in addition, they are almost completely null when an external continuum is included (for either the monomer or a cluster). These results should support the validity of the analysis

Table 8. Paramagnetic and Diamagnetic Shieldings (ppm) and NBO Nitrogen Lone Pair Natural Population (NP(lp)) for Diazines and Water–Diazine Clusters in Vacuo (VAC) and in the Presence of an External Continuum (IEF)^a

	VAC			IEF		
	m	+1w	+2w	m	+1w	+2w
			Pyridazine			
NP(lp)	1.939	1.921	1.922 (1.933)	1.943	1.912	1.912 (1.924)
σ_{is}^p	-513.52	-513.09	-496.41 (-504.49)	-482.44	-487.20	-474.83 (-475.21)
σ_{is}^d	296.58	325.07	318.31 (313.20)	296.90	324.80	319.33 (313.95)
			Pyrimidine			
NP(lp)	1.919	1.908	1.909	1.924	1.899	1.900
σ_{is}^p	-373.88	-384.09	-383.21	-363.159	-376.34	-375.97
σ_{is}^d	296.43	322.21	320.41	296.811	322.83	320.69
			Pyrazine			
NP(lp)	1.923	1.911	1.912	1.928	1.903	1.904
σ_{is}^p	-409.07	-412.36	-418.97	-399.32	-408.62	-412.69
σ_{is}^d	290.22	314.38	314.89	290.48	317.20	316.64

^a For pyridazine 2w clusters two values corresponding to the two nonequivalent nitrogens are reported.

based on the paramagnetic term only to explain differences between smaller and larger clusters on one hand, and between gas-phase and solvated results on the other hand: a warning is, in contrast, necessary when we extend such an analysis to the monomers, as in these cases the changes in the diamagnetic parts can be important.

To investigate the effects of H-bonding, we compare (both in the series of gas-phase results and in the parallel one with an external continuum) lone pair occupancies of monomers and clusters: a significant decrease is found for the one-water cluster, which is then partially canceled on passing to the two-water analogue. This electronic charge transfer is sufficiently well correlated to the prediction by eq 1 for the paramagnetic shielding: removing electron population from the lone pair orbital should cause the corresponding electron orbital to shrink toward the nucleus, increasing the $\langle r^{-3} \rangle$ term and thus the magnitude of the paramagnetic contribution. As a matter of fact, in both pyridazine and pyrimidine, σ_{is}^p shows the most negative value corresponding to the 1w clusters.

A different analysis involves the comparison between isolated and “solvated” (IEF) systems. For all the three monomers, the inclusion of a continuum dielectric induces a significant increase in the nitrogen lone pair population, which means more diffuse orbitals, a smaller $\langle r^{-3} \rangle$ term, and thus a less negative σ_{is}^p . The analysis becomes less simple on passing to clusters: adding the continuum reduces the lone pair population of each cluster (indicating a stronger charge transfer from nitrogen lone pair to H-bonded waters, as already noted in the previous analysis on pyridazine, see Table 3); however, this is reflected not in a more negative σ_{is}^p , as expected from considerations on the $\langle r^{-3} \rangle$ term but, in contrast, in a net decrease of its absolute value.

The reasons for this can be various. For example, it can happen that, on passing from isolated to solvated clusters, the dominant term in determining the paramagnetic shielding becomes ΔE ; in fact, if we assume that all other electronic transition energies are much larger than $\Delta E_{n\pi^*}$ and therefore make a negligible contribution to σ_{is}^p , the observed decrease in the paramagnetic shielding in the presence of the external continuum can be explained in terms of the parallel net increase of the $n \rightarrow \pi^*$ transition energy (see Table 2).

In a more general analysis, all the nuclear shielding results show that inclusion of long-range nonspecific interactions (here represented by the continuum) amplifies H-bond effects due to a stronger interaction between the diazine and the bonded water molecules. This reinforcing effect of the field induced by the external continuum confirms what was found in the previous analysis on electronic transitions and shows that both properties ($n \rightarrow \pi^*$ transition and nitrogen shielding) are affected in a similar way by the solvent. We also observe that an indirect confirmation of this synergic (or cooperative) action of H-bond and polar effects is represented by pyridazine–2w clusters, in which the presence of the continuum reduces the nonequivalence of the two nitrogens (the differences in both the H...N distances and the shieldings for the two nitrogens is more than halved on passing from the isolated 2w cluster to the solvated one).

4.2. Final Comments and Comparison with an Empirical Approach. The results reported in the previous sections can be collectively analyzed in terms of a final correlation plot between calculated and experimental data, where the calculated data are those obtained using a larger cavity and (in the case of water) the IEF 2w clusters. The plot is reported in Figure 2, together with the line resulting from a linear fitting.

From the comparison of Figure 2 with Figure 1, it appears evident that an improvement is achieved by introducing a combination of refinements in the continuum solvation model so as to take into account both nonelectrostatic effects (through a larger cavity) and, in the case of water, more specific H-bonding interactions (through 2w clusters). The correlation is now very good (the correlation coefficient is 0.99932), and all the major changes induced by solvent polarity and those exerted by solvent to solute hydrogen bonding are very well represented. Even so, a more detailed analysis of the line equation,

$$\Delta\sigma_{\text{exp}} = [0.8621(\pm 0.010)\sigma_{\text{calc}} + 144.58(\pm 1.35)] \pm 1.81 \text{ ppm}$$

indicates that the calculations overestimate the magnitude of the shieldings and that the overall standard deviation of about ± 1.8 ppm does not allow one to go into a very detailed numerical interpretation of small effects; however, even in the

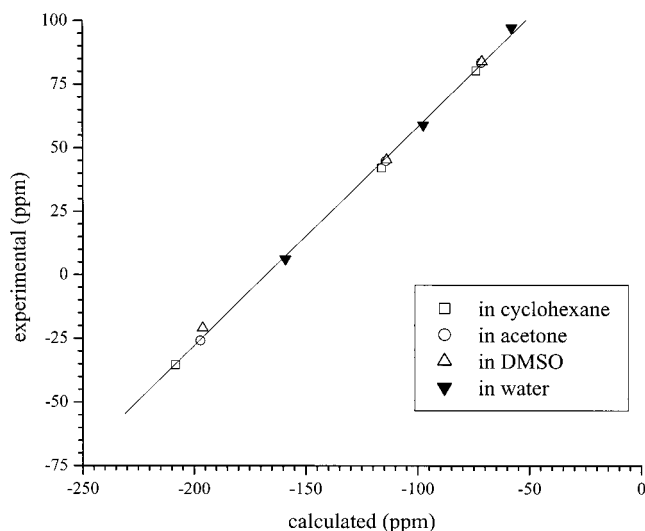


Figure 2. Experimental and B3LYP/GIAO/6-311+G(d,p) isotropic N nuclear shielding plot of diazines in various solutions. The calculated results are obtained with the IEF continuum model and larger cavities (see text for details); in the case of water solution, two H-bonded water molecules are explicitly included. Experimental data are reported with respect to neat liquid nitromethane.

cases where the polarity effects on the shieldings are relatively small, the signs and orders of magnitude are predicted correctly.

The final results summarized in Figure 2 can be further evaluated by a comparison with an approach based on the so-called solvent empirical parameters.

In brief, this approach, originally proposed by Kamlet, Taft, and co-workers,²⁸ does not involve quantum mechanical or other types of calculations, but it introduces a numerical treatment of experimental data obtained for a given reference system to obtain an estimate of solvent effects on various properties. Its generalization to the study of the solvent effect on nitrogen nuclear shielding in diazines has been proposed by Witanowski et al.²⁴ The analysis is the following: in order to separate the various nitrogen shielding contributions, a four-parameter master equation is introduced to relate the shielding in any solvent X to that measured in a reference solvent (here cyclohexane) through additive terms related to some solvent properties. The working expressions yields

$$\sigma(X) = \sigma(\text{cyc}) + s(\pi^* + d\delta) + a\alpha + b\beta \quad (2)$$

where π^* is an index of solvent polarity–polarizability which measures the ability of the solvent to stabilize a charge or a dipole by virtue of its dielectric effects, α represents solvent hydrogen bond donor strength, β gives the hydrogen bond acceptor strength, δ is a correction for polychlorinated and/or aromatic solvents, and s , d , a , and b are the corresponding responses of the appropriate solute molecular property (here the shielding) to the relevant solvent property. These coefficients are obtained through a least-squares fitting on various solvents.

The solvent parameters employed by Witanowski et al. for diazine are reported in Table 9, while the corresponding solvent effects (with respect to cyclohexane) are summarized in Table 10; parameters for water are reported between parentheses as less certain.

Table 9. Kamlet and Taft Parameters for Diazines in Acetone and Water Solutions^a

	α	β	π^*	δ
acetone	0.07	0.48	0.72	0
H ₂ O	(1.13)	(0.18)	(1.09)	0
	a	b	s	d
pyridazine	20.85 ± 0.94	−0.33 ± 1.47	12.99 ± 1.37	0.04 ± 0.49
pyrimidine	8.21 ± 0.31	−0.92 ± 0.49	4.09 ± 0.46	0.08 ± 0.12
pyrazine	7.26 ± 0.32	−0.89 ± 0.57	3.73 ± 0.47	0.01 ± 0.14

^a Data are from ref 24.

Table 10. Polarity–Polarizability ($\delta\sigma^\pi$) and H-Bond ($\delta\sigma^\alpha$) Contributions (in ppm) to Solvent Shift on Nitrogen Shielding for Diazines in Acetone and Water Solutions As Obtained from Eq 2

	pyridazine		pyrimidine		pyrazine	
	acetone	H ₂ O	acetone	H ₂ O	acetone	H ₂ O
$\delta\sigma^\pi$	9.4	14.2	2.9	4.5	2.7	4.1
$\delta\sigma^\alpha$	1.5	23.5	0.6	9.3	0.5	8.2
$\delta\sigma^{\text{tot}}$	10.9	37.7	3.5	13.8	3.2	12.3

The results given in Table 10 give various elements of comparison with what was obtained in our calculations. First they show that, for all diazines, both the term a , which represents the response of the nitrogen shielding to the solvent hydrogen bond donor strength, and the term s , which corresponds to the effect of solvent polarity–polarizability on the solute nitrogen shielding, are positive; this confirms our previous statement that the two effects induce variations in the same directions. In addition, these results show that, for each diazine in water, the solvent polarity–polarizability contribution (indicated as $\delta\sigma^\pi$ in Table 10) to the shift is correlated to the hydrogen bond contribution $\delta\sigma^\alpha$, the former being almost one-half of the latter; this indicates that polarizability and H-bond effects synergically interact exactly as we have found by analyzing NBO results on the solvated clusters. For a more correct analysis, it has to be noted that eq 2 does not contain any explicit “van der Waals term”, and thus eventual effects due to dispersive interactions are indirectly included in the s and a coefficients (through the fitting procedure): the resulting contributions to the shift are thus not pure polarity–polarizability and H-bond, respectively.

5. Conclusions

In this work we applied a sequence of solvation models (continuum, discrete, continuum + discrete) to study solvent effects on the $n \rightarrow \pi^*$ transition and nitrogen nuclear shielding of diazines in different solvents and, more in particular, in water. Such alternation/combination of different models has been required to study the complex nature of solute–solvent interactions when both long-range “polar” and shorter-range specific H-bond effects are active. In these cases, in fact, we showed that a pure continuum model fails to describe the total solvent effect (we note that the performances of continuum models are here tested in terms of the changes induced on two quantities, the electronic transition and the nuclear shielding, which are known to be very sensitive to even small modifications of electronic and/or nuclear charge distributions). In the literature, there are many examples of computational studies which, on the basis of similar considerations, introduce MD or Monte Carlo simulations to get a more correct description. The large number of molecules generally involved in this kind of analysis,

(28) Kamlet, M. J.; Abboud, J. L. M.; Taft, R. W. *Prog. Phys. Org. Chem.* **1980**, *13*, 485.

however, prevents one from doing very accurate calculations of the property of interest (usually semiempirical or low-level QM methods or mixed QM/MM approaches are exploited). In any case, the important result that comes from these studies is that very large clusters of solute–solvent molecules (going far beyond the first solvation shell) have to be considered to get the full solvent effect.^{3,4}

With this work, and the previous one on acetonitrile,¹⁵ we have tried to consider the problem from a different point of view by introducing a two-step procedure. The first step is an analysis of the solvent-induced modifications on the property of interest, which are obtained through a solvation continuum model. At this level it is fundamental that the continuum model is as accurate as possible: in our case this is realized through the IEF–PCM approach. Such model, in fact, can be coupled to high-level quantum mechanical calculations through an effective Hamiltonian in which a perturbation operator directly dependent on the solute wave function is introduced to represent the electrostatic interactions and a molecularly shaped cavity is used. On the basis of the results obtained in this continuum framework (and, in particular, of possible failures), the following step is defined to include all those aspects of the solvation phenomenon which are still missing (or are only partially accounted for). In the numerical practice, this means to introduce completely different approaches, and to combine them in order to get an accurate evaluation of the solute response properties and of the way these are modified by the environment.

In the two papers, the attention has been focused on different versions of the same phenomenon (mainly the effects due to protic solvents on selected properties of H-acceptor solutes). Here we have analyzed a strong H-donor–acceptor solute–solvent couple (water–diazine), while in the previous study the focus was on the far weaker CHCl_3 –acetonitrile interactions: the differences between the two systems required the use of different approaches, but the two analyses are strongly connected, and they are better appreciated in a unified picture.

The main idea followed in both works is to explore different theoretical methods to explain solvent effects in terms of clear physical concepts related to intermolecular interactions, and to give a valid confirmation of the analysis derived from the calculations through a quantitative comparison with experimental data on various properties. Such studies have both involved protic solvents and H-bond acceptor solutes, as the complex nature of such systems allows a more complete (and more interesting) analysis on limitations and potentialities of theoretical models aiming at describing solvent effects. In conjunction, the two works have shown that a single protocol of analysis cannot be found. However, some general rules seem to come out: (1) H-bonding solute–solvent systems require a combination of different solvation approaches which has to be chosen in relation to the nature, and the strength, of the H-bond interactions on one hand, and to the type of analysis to be done on the other hand; (2) if this analysis is focused on molecular response properties, then the solute system has to be described at an accurate electronic level, otherwise a complete confidence in the results cannot be obtained; (3) the solvent (or a part of it) can be treated at a lower level but only if all the interactions have been included in the model in a balanced way.

These three apparently simple rules can become hard to realize in the computational practice: our studies, however, show that considerations on the chemical nature of the molecular system when combined with a physical analysis of the molecular property under scrutiny can be used to define simple but effective protocols. In the previous paper, we have shown that, for low-polarity solvents giving a weak H-bonding with the solute (like acetonitrile in CHCl_3), a statistical analysis on “combined” or “hybrid” calculations (in our case realized through the ONIOM²⁹ formalism) on medium-dimension clusters obtained through MD simulations is a good approximation and that, in those systems in which underestimation of the so-called bulk effect is found, further improvements can be obtained by including an external continuum dielectric. Here we have shown that, for more polar and stronger H-bonding solute–solvent systems (like diazines in water), a sufficiently accurate description can be obtained with far smaller (in the number of solvent molecules) clusters but only on the condition that (i) H-bonded structures are introduced through high-level quantum mechanical optimization techniques and (ii) the bulk effect is taken into account through an accurate continuum model both in the evaluation of the geometries and of the response properties.

It is important to note that the results of both studies confirm one of the main points predicted by completely different approaches (in particular those in which the microscopic structure of solvent molecules in the solution is taken into account): namely, that H-bonding effects, to be correctly described, need the inclusion of the long-range interactions due to solvent molecules far beyond the first solvation shells (i.e., the bulk).

The limited amount of data we have tested so far (as concerns both solute–solvent systems and molecular properties) cannot give a definitive answer on the still open problem of the best way to couple different solvation models in order to take into account all possible aspects related to H-bonding solute–solvent systems. However, the results we have presented in these two studies can be considered as the beginning of a multilayer analysis on the state of the art of modern theoretical solvation models and on the way these can answer the main questions concerning the physical nature and the computational representation of the solvation phenomenon. Many further confirmations of the two alternative methodological schemes we have proposed are surely required, as are extensions to other types of solute–solvent couples (not dominated by polar or H-bonding interactions) and to other molecular properties: development in these directions is already in progress.

Supporting Information Available: Tables listing B3LYP/6-31+G(d,p) geometries of the compounds described herein and the energies of diazines and diazine–water clusters (PDF). This material is available free of charge via the Internet at <http://pubs.acs.org>.

JA0118542

- (29) (a) Svensson, M.; Humbel, S.; Froese, R. D. J.; Matsubara, T.; Sieber, S.; Morokuma, K. *J. Phys. Chem.* **1996**, *100*, 19357. (b) Humbel, S.; Sieber, S.; Morokuma, K. *J. Chem. Phys.* **1996**, *16*, 1170. (c) Maseras, F.; Morokuma, K. *J. Comput. Chem.* **1995**, *16*, 1170. (d) Vreven, T.; Morokuma, K. *J. Comput. Chem.* **2000**, *16*, 1419.